Journal of Dental Research
2023, Vol. 102(1) 103–115

Article reuse guidelines:
sagepub.com/journals-permissions
DOI: 10.1177/00220345221123256
journals.sagepub.com/home/jdr

TRAF3IP2–IL-17 Axis Strengthens the Gingival Defense against Pathogens

J. Zhang[1,2*], L. Sun[3,4*], M.H.H. Withanage[5], S.M. Ganesan[1,2], M.A. Williamson[1,2], J.T. Marchesan[6], Y. Jiao[6], F.R. Teles[7], N. Yu[8], Y. Liu[9], D. Wu[6,9], K.L. Moss[6], A.K. Mangalam[10], E. Zeng[5], Y.L. Lei[11], and S. Zhang[1,2]

Abstract

Recent genome-wide association studies have suggested novel risk loci associated with periodontitis, which is initiated by dysbiosis in subgingival plaque and leads to destruction of teeth-supporting structures. One such genetic locus was the tumor necrosis factor receptor–associated factor 3 interacting protein 2 (*TRAF3IP2*), a gene encoding the gate-keeping interleukin (IL)–17 receptor adaptor. In this study, we first determined that carriers of the lead exonic variant rs13190932 within the *TRAF3IP2* locus combined with a high plaque microbial burden was associated with more severe periodontitis than noncarriers. We then demonstrated that TRAF3IP2 is essential in the IL-17–mediated CCL2 and IL-8 chemokine production in primary gingival epithelial cells. Further analysis suggested that rs13190932 may serve a surrogate variant for a genuine loss-of-function variant rs33980500 within the same gene. *Traf3ip2* null mice (*Traf3ip2*$^{-/-}$) were more susceptible than wild-type (WT) mice to the *Porphyromonas gingivalis*–induced periodontal alveolar bone loss. Such bone loss was associated with a delayed *P. gingivalis* clearance and an attenuated neutrophil recruitment in the gingiva of *Traf3ip2*$^{-/-}$ mice. Transcriptomic data showed decreased expression of antimicrobial genes, including *Lcn2*, *S100a8*, and *Defb1*, in the *Traf3ip2*$^{-/-}$ mouse gingiva in comparison to WT mice prior to or upon *P. gingivalis* oral challenge. Further 16S ribosomal RNA sequencing analysis identified a distinct microbial community in the *Traf3ip2*$^{-/-}$ mouse oral plaque, which was featured by a reduced microbial diversity and an overabundance of *Streptococcus* genus bacteria. More *P. gingivalis* was observed in the *Traf3ip2*$^{-/-}$ mouse gingiva than WT control animals in a ligature-promoted *P. gingivalis* invasion model. In agreement, neutrophil depletion resulted in more local gingival tissue invasion by *P. gingivalis*. Thus, we identified a homeostatic IL-17-TRAF3IP2-neutrophil axis underpinning host defense against a keystone periodontal pathogen.

Keywords: periodontitis, genomics, cytokines, chemokines, bone loss, microbiome

Introduction

Periodontitis, as a complex trait disease, is associated with risk alleles with varying effect sizes that have been reported by several genome-wide association (GWA) studies (Divaris et al. 2013; Offenbacher et al. 2016). Through a gene-set enrichment GWA analysis in the Atherosclerosis Risk in Communities (ARIC) participants, we recently reported several genes in which the combined overall single-nucleotide polymorphism (SNP) variants were significantly associated with several periodontal complex traits (PCTs) defined by clinical disease classification and biological intermediates, including microbial and inflammatory characteristics (Offenbacher et al. 2016). For example, the combined SNP variants across the tumor necrosis factor receptor–associated factor 3 interacting protein 2 (*TRAF3IP2*, *ACT1*, or *CIKS*) gene were significantly associated with PCT3, which was characterized by a high loading of gingival crevicular fluid interleukin (IL)–1β level and *Aggregatibacter actinomycetemcomitans* in subgingival plaque (Offenbacher et al. 2016).

TRAF3IP2 encodes a nonredundant adaptor protein for the IL-17 receptor (IL-17R) that mediates IL-17 responses in several cell types (Huang et al. 2007; Boisson et al. 2013; Ha et al. 2014; Wu et al. 2014). IL-17 family members, including IL-17(A), IL-17E (IL-25), and IL-17F, rely on TRAF3IP2 to phosphorylate TRAF6 and initiate downstream signaling

[1]Iowa Institute of Oral Health Research, University of Iowa College of Dentistry, Iowa City, IA, USA
[2]Periodontics, University of Iowa College of Dentistry, Iowa City, IA, USA
[3]Department of Microbiology & Immunology, School of Medicine, University of North Carolina at Chapel Hill, Chapel Hill, NC, USA
[4]Lineberger Comprehensive Cancer Center, School of Medicine, University of North Carolina at Chapel Hill, Chapel Hill, NC, USA
[5]Division of Biostatistics and Computational Biology, University of Iowa College of Dentistry, Iowa City, IA, USA
[6]Department of Periodontology, Adams School of Dentistry, University of North Carolina at Chapel Hill, Chapel Hill, NC, USA
[7]Department of Basic & Translational Sciences, University of Pennsylvania School of Dental Medicine, Philadelphia, PA, USA
[8]The Forsyth Institute, Cambridge, MA, USA
[9]Department of Biostatistics, Gillings School of Global Public Health, University of North Carolina at Chapel Hill, Chapel Hill, NC, USA
[10]Department of Pathology, University of Iowa College of Medicine, Iowa City, IA, USA
[11]Department of Periodontics & Oral Medicine, University of Michigan School of Dentistry, Ann Harbor, MI, USA
*Authors contributing equally to this article.

A supplemental appendix to this article is available online.

Corresponding Author:
S. Zhang, Iowa Institute of Oral Health Research, Periodontics Department, University of Iowa College of Dentistry, Room 401 Dental Science Building, 801 Newton Road, Iowa City, IA 52242, USA.
Email: shaoping-zhang@uiowa.edu

events (Gu et al. 2013). IL-17 stimulation promotes the activation of NF-κB or mitogen-activated protein (MAP) kinases, which are essential in controlling the magnitude of immune induction (Gu et al. 2013). Several variants within the *TRAF3IP2* gene locus have been associated with inflammatory diseases such as psoriasis, inflammatory bowel disease, and mucocutaneous candidiasis (Ellinghaus et al. 2010; Hüffmeier et al. 2010; Ciccacci et al. 2013; Marujo et al. 2021). A missense mutation within the *TRAF3IP2* locus was associated with an inferior protection against *Candida albicans* (Boisson et al. 2013). The loss-of-function *TRAF3IP2* variants that abolish the homeostatic activity of this IL-17R adaptor protein were associated with a compensatory hyperproduction of other T-helper cell (Th)17 cytokines, including IL-17F, IL-21, and IL-22 or dampened mucosal barrier defense (Sønder et al. 2012; Wang et al. 2013).

As the role of TRAF3IP2 in periodontal disease has not been delineated yet, the association between the combined overall variants within the *TRAF3IP2* locus and the PCT3 periodontitis trait prompted us to conduct an in-depth mechanistic study on the role of TRAF3IP2 in regulating gingival barrier function. Here we report that TRAF3IP2-mediated homeostatic neutrophil recruitment is critical for maintaining host defense to avert *Porphyromonas gingivalis*–induced bone loss. We also show that the lead or top-ranked (smallest *P* value) exonic SNP rs13190932 within the *TRAF3IP2* locus may serve as surrogate for a loss-of-function rs33980500 variant, leading to an impaired IL-17 signaling.

Materials and Methods

Detailed description of materials and methods is included in the Appendix.

Results

Exonic Variant rs13190932 within the TRAF3IP2 *Locus Was Associated with Periodontitis*

We previously reported that the overall variants across the *TRAF3IP2* gene locus were significantly associated with PCT3 (Offenbacher et al. 2016; Zhang et al. 2020). When variants within the *TRAF3IP2* locus were analyzed individually for association with PCT3, the lead coding nonsynonymous variant was rs13190932 (G/A), which is located in the second exon of the *TRAF3IP2* gene ($P = 8.43 \times 10^{-7}$) (Zhang et al. 2020). The variant A allele has an overall frequency of 0.058 in the population and is more common in Caucasians, with a frequency of 0.061. Among ARIC subjects who had a complete periodontal exam and genotyping data, homozygous carriers ($n = 15$) of the rare allele (A/A or "2.2") for rs13190932 had significantly more prevalent disease, defined by the percentage of interproximal sites with the attachment loss equal to or greater than 3 mm, than noncarriers ($n = 4{,}152$) (G/G or "1.1") or heterozygous participants ($n = 599$) (G/A or "1.2") (Fig. 1A).

We also found that subjects with a higher microbial burden (top 25th percentile) of the "red complex" bacteria (*P. gingivalis*, *Tannerella forsythia*, and *Treponema denticola*) (Fig. 1B), the "orange complex bacteria" (*Campylobacter rectus*, *Fusobacterium nucleatum*, *Prevotella intermedia*, and *Prevotella nigrescens*) (Fig. 1C), and *A. actinomycetemcomitans* (Fig. 1D) manifested significantly more sites with severe disease than subjects with a lower plaque pathogen burden (bottom 75th percentile) regardless of *TRAF3IP2* genotypes, which was well expected. Notably, we observed that in subjects with a higher pathogen burden, the presence of 1 or 2 copies of variant A allele at rs13190932 was significantly associated with a more severe disease phenotype (Fig. 1B–D, Appendix Fig. 1). However, in subjects with a lower plaque pathogen burden, the impact of the variant was modest. These data suggest that rs13190932 (A) variant carriers are more susceptible than nonvariant allele carriers to the high plaque microbial burden–associated severe periodontitis.

IL-17–TRAF3IP2–Mediated Response in Gingival Epithelial Cells

TRAF3IP2 and IL17R are predominantly expressed in epithelial cells in both healthy and periodontitis gingival biopsy specimens (Fig. 2A). We reported that TRAF3IP2 was indispensable for the IL-17–induced neutrophil specific chemokine CXCL1 expression in primary human gingival epithelial cells (pHGEs) (Sun et al. 2020). Here we found that an efficient knockdown of *TRAF3IP2* by shRNA1 abrogated the IL-17–induced transcription of *IL8* (*CXCL8*), *CCL2*, and *IL6* in pHGEs (Fig. 2B). However, transcription of the matrix metalloproteinase-3 (*MMP3*) was not affected by the IL-17–TRAF3IP2 axis. The measurement of proteins in the supernatant confirmed the transcriptional data (Fig. 2C). TRAF3IP2 knockdown also inhibited the production of granulocyte macrophage colony-stimulating factor (GM-CSF), an important upstream signal for myeloid cell proliferation. We further identified that the activation of the canonical NF-κB pathway, as assayed by p-NF-κBp65, was involved in the IL-17–TRAF3IP2 signaling in pHGEs (Appendix Fig. 2A). Pretreatment of pHGEs with Bay 11-7082, an NF-κB inhibitor, blocked more than 50% of the *CXCL1*, *IL8*, and *IL6* induction by IL-17 as compared to dimethyl sulfoxide (DMSO)–treated cells (Appendix Fig. 2B).

The rare allele (A) frequency for rs13190932 is in high linkage disequilibrium ($D' = 1$, $r^2 = 0.90$) in North European descendants with rs33980500 (C/T), another missense nonsynonymous variant within the *TRAF3IP2* locus (Fig. 2D) (Myers et al. 2020). Therefore, we assessed the functional variant effect of both SNPs on the IL-17 response. Cells transfected with the *TRAF3IP2* clone bearing the variant rs13190932 (A) stimulated by IL-17 resembled the cells transfected with the nonvariant *TRAF3IP2* clone, while the variant rs33980500 (T) significantly blocked the transcription of *CXCL1* and *IL8* in comparison to the nonvariant transfected cells (Fig. 2E). The cellular response to the variant haplotype with both variants

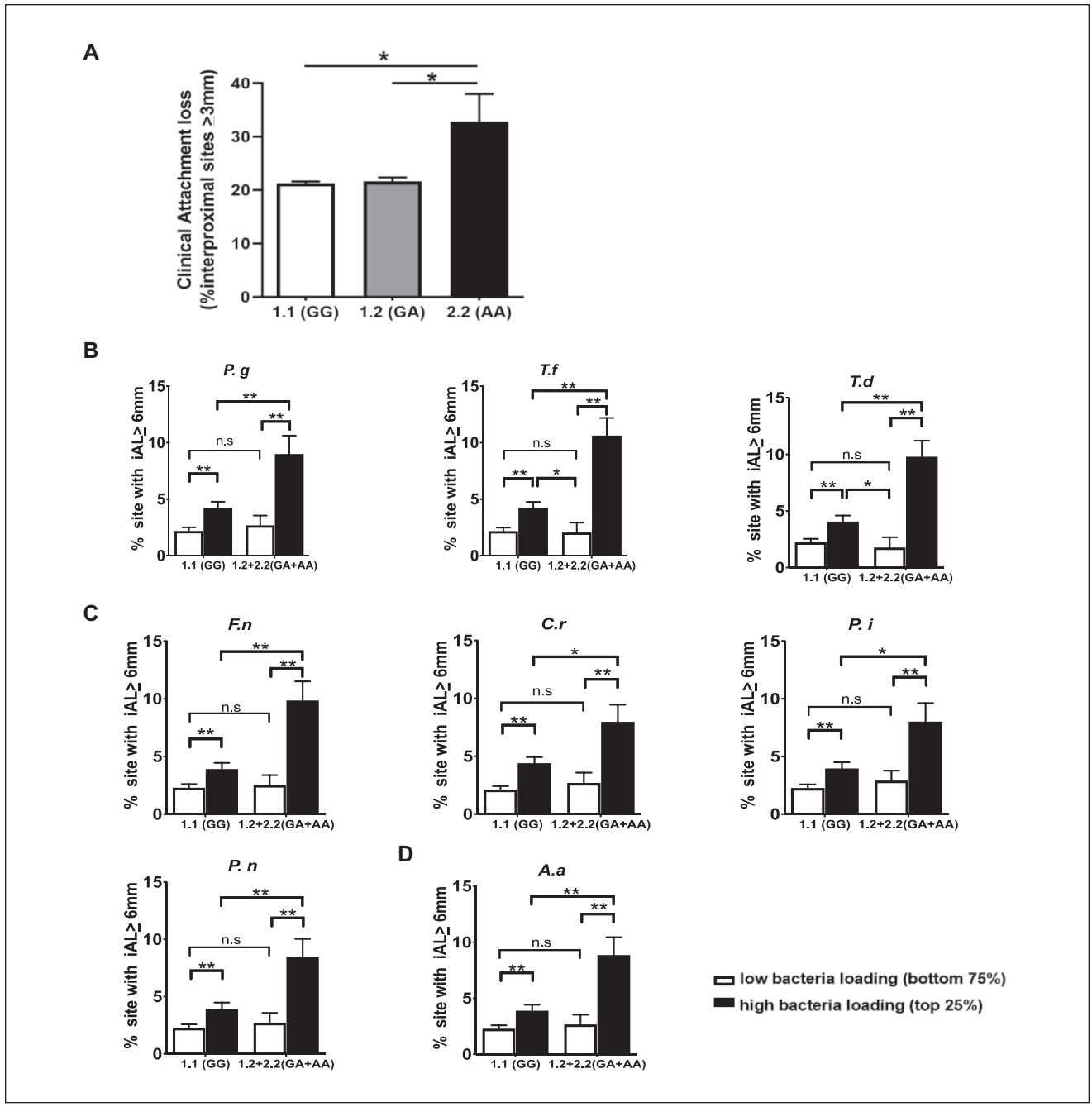

Figure 1. *TRAF3IP2* single-nucleotide polymorphism rs13190932 is associated with periodontal disease. (**A**) Subjects ($n = 15$) with homozygous variant allele (A/A or "2.2") at the variant site presented significantly more disease activity, as reflected by the extent (%) of interproximal sites exhibiting 3 mm or above in clinical attachment loss, than participants ($n = 599$) with the heterozygous genotype (G/A or "1.2") or nonvariant carriers (G/G or "1.1") ($n = 4,152$) in the Atherosclerosis Risk in Communities (ARIC) subjects. (**B**) Microbial levels of 8 common periodontitis-associated bacteria assessed by checkerboard DNA–DNA hybridization in ARIC subjects ($n = 1,173–1,181$) were dichotomized into either a high microbial burden (top 25th percentile) or low burden (bottom 75th percentile). Among ARIC participants with a high microbial burden of "red complex" bacteria, *Porphyromonas gingivalis* (*P.g*), *Tannerella forsythia* (*T.f*), and *Treponema denticola* (*T.d*), variant carriers with 1 (1.2) or 2 copies (2.2) of rs13190932 within the *TRAF3IP2* locus had significantly more severe periodontitis-involved sites as reflected by the percentage of interproximal attachment loss 6 mm or greater than noncarriers (1.1) with the same level of pathogens. (**C**) Variant carriers with a high "orange complex" bacteria loading, including *Fusobacterium nucleatum* (*F.n*), *Campylobacter rectus* (*C.r*), *Prevotella intermedia* (*P.i*), and *Prevotella nigrescens* (*P.n*) or (**D**) *Aggregatibacter actinomycetemcomitans* (*A.a*), presented significantly more severe diseased sites than noncarriers with the same pathogen level. $^*P < 0.05$; $^{**}P < 0.01$; n.s, not significant. n (1.1) = 1,054–1,062; n (1.2+2.2) = 119. Mean ± standard error (SEM) is shown.

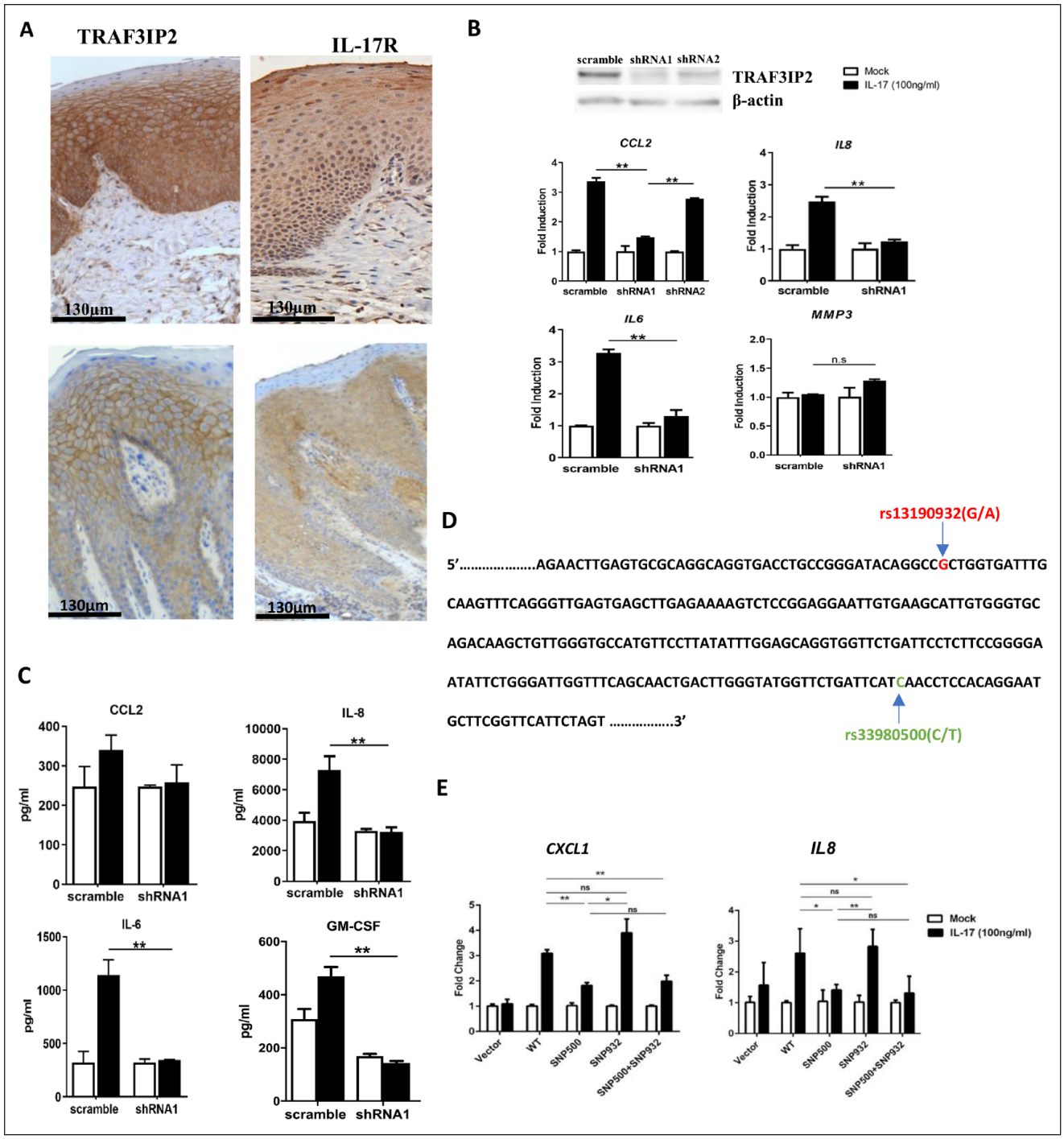

Figure 2. rs13190932 may serve as a proxy for the exonic rs33980500 variant within the *TRAF3IP2* locus in mediating chemokine response stimulated by interleukin (IL)–17 in primary human gingival epithelial cells (pHGEs). (**A**) The TRAF3IP2 molecule predominately expressed in gingival epithelia in a periodontitis-free human gingival biopsy specimen (upper panel) and approximated with the IL-17 receptor as stained by immunohistochemistry. Similarly, the expression of the TRAF3IP2 and IL-17 receptor was also predominantly present in the gingival epithelia in periodontitis lesional tissues (lower panel). (**B**, upper panel) The endogenous TRAF3IP2 expression was knocked down (KD) by different short hairpin (sh)RNA-lentiviral vectors in pHGEs. Cells transduced with a scramble shRNA vector served as a control. The knockdown efficiency was higher in the shRNA1 vector as determined by Western blotting. (**B**, lower panel) Scramble shRNA transduced or *TRAF3IP2* KD pHGEs were challenged with 100 ng/mL IL-17 for 3 h and *CCL2*, *IL8*, *IL6*, and *MMP3* messenger RNA (mRNA) levels were quantified by quantitative reverse transcriptase polymerase chain reaction (RT-qPCR). (**C**)The protein level of CCL2, IL-8, IL-6, and granulocyte macrophage colony-stimulating factor (GM-CSF) was measured 8 h after IL-17 challenge. (**D**) Partial DNA sequence that includes the variant sites rs13190932 and rs33980500 within the second exon of the *TRAF3IP2* gene is shown. Both variants are highlighted in color. (**E**) HeLa cells transfected with wild-type complementary DNA clones of *TRAF3IP2* or clones bearing variant rs13190932 and/or rs33980500 were stimulated with 100 ng/mL IL-17 for 3 h. Cells transfected with the empty vector served as a control. The mRNA level of *CXCL1* and *IL8* was quantified by RT-qPCR. *$P<0.05$; **$P<0.01$; ns, indicates not significant. All *in vitro* experiments were performed at least twice in triplicate. Data from 1 representative experiment are shown. Mean ± standard deviation (SD) is shown.

was similar to the response of the single rs33980500 variant. These data suggest that, rather than rs13190932, rs33980500 is a loss-of-function variant and might be a genuine periodontal disease–associating variant.

Traf3ip2$^{-/-}$ *Mice Were More Susceptible to* P. gingivalis*–Induced Periodontitis That Is Associated with a Compromised Mucosal Defense Transcriptomic Signature*

We next employed a pathogen-induced oral infection model to characterize the role of the homeostatic TRAF3IP2-mediated IL-17 pathway in periodontitis (Fig. 3A). *Traf3ip2*$^{-/-}$ mice that were orally challenged with the *P. gingivalis* A7436 strain presented significantly more alveolar bone loss than *Traf3ip2*$^{-/-}$ mice challenged with Carboxymethylcellulose CMC (control) (Fig. 3B). However, no significant difference was found between *P. gingivalis* A7436 and CMC-challenged WT mice. The resistance to *P. gingivalis*–induced bone loss in the C57BL/6 background WT mice was consistent with previous reports (Baker et al. 2000; Sun et al. 2020). The average net bone loss as the bone level subtracting the CMC challenged from the *P. gingivalis*–challenged *Traf3ip2*$^{-/-}$ mice was also significantly higher than the net bone loss calculated from WT mice (Fig. 3B). This net bone loss reflects the strain-specific susceptibility to *P. gingivalis*–induced bone loss.

We next compared the neutrophil recruitment in *Traf3ip2*$^{-/-}$ mouse gingiva to the recruitment in WT mice. Although *P. gingivalis* challenge resulted in a significant increase in neutrophils as compared to CMC treatment in WT mice, significantly fewer Ly6G^{+} neutrophils were present in the gingival tissue from *Traf3ip2*$^{-/-}$ mice than WT mice 2 d after the completion of the *P. gingivalis* challenge (Fig. 3C). In addition, the residual plaque *P. gingivalis* was significantly higher in *Traf3ip2*$^{-/-}$ mice than WT mice at the same time point (Fig. 3D).

However, in a ligature-induced periodontitis mouse model, the bone level was not significantly different between WT and *Traf3ip2* null mice (Appendix Fig. 3). Taken together, our *in vivo* data suggest that the loss of the homeostatic IL-17–TRAF3IP2 pathway predisposes mice to the *P. gingivalis*–induced alveolar periodontal bone loss, impaired neutrophil recruitment in gingiva, and delayed the clearance of *P. gingivalis*.

We also assessed the IL-17 pathway-associated transcriptomic profile in *Traf3ip2*$^{-/-}$ mouse gingiva at different stages upon *P. gingivalis* challenge (Fig. 3E). We did not observe significant changes in transcripts of chemokine or cytokine genes, including *Cxcl1*, *Ccl2*, *Gmcsf*, and *Il6*, in the *Traf3ip2*$^{-/-}$ mouse gingiva as compared to the WT control animals. Instead, we found that the transcription of several epithelial marker genes and those associated with epithelial barrier function, including keratin 1 (*Krt1*), Kruppel-like factor 4 (*Klf4*), occludin (*Ocln*), desmocollin 1 (*Dsc1*), desmoglein 1 (*Dsg1*), and *Filaggrin*, was significantly lower in *Traf3ip2* null mouse gingiva than WT mice either at the baseline or upon *P. gingivalis* challenge (Fig. 3F). Transcription of genes closely associated with antimicrobial defense, including lipocalin 2 (*Lcn2*), *S100a8*, *S100a9*, and β defensins (*Defb1* and *Defb4*), was also significantly diminished in the knockout (KO) mouse gingiva (Fig. 3G). The transcription of *Runx2*, an osteoblast differentiation marker, was significantly lower in *Traf3ip2*$^{-/-}$ mice upon *P. gingivalis* challenge than WT mouse gingiva. Such a transcriptomic signature in the KO animals suggested a breach in both a physical and an immune barrier in the gingiva of *Traf3ip2*$^{-/-}$ mice that were susceptible to *P. gingivalis*–induced alveolar bone loss.

Absence of IL-17–TRAF3IP2 Pathway Was Associated with a Distinct Oral Microbial Profile

Through the 16S ribosomal RNA (rRNA) sequencing, we found that the oral plaque from *Traf3ip2*$^{-/-}$ mice had a lower compositional (α) diversity at the baseline and during *P. gingivalis* oral challenge than the WT plaque samples (Appendix Fig. 4). The β-diversity from all oral plaque samples clearly illustrated a unique microbial signature in *Traf3ip2*$^{-/-}$ oral plaque (Fig. 4A). We observed that the relative abundance of taxonomic groups of bacteria was drastically different between the KO and WT mice (Fig. 4B). For example, *Streptococcus* was more enriched in oral plaque from *Traf3ip2*$^{-/-}$ mice at any given time point than the WT mice samples. Further Linear discriminant analysis Effect Size LEfSe analysis indicated that bacteria from the *Corynebacterium* and *Staphylococcus* genera were significantly more abundant in WT plaque, while the *Streptococcus* genus was significantly more enriched in *Traf3ip2*$^{-/-}$ mice prior to or upon *P. gingivalis* challenge (Fig. 4C, D).

The high abundance of *Streptococcus* genus bacteria, observed in *Traf3ip2*$^{-/-}$, may help *P. gingivalis* to colonize in plaque (Simionato et al. 2006). Through a fluorescence *in situ* hybridization (FISH) assay, we found that *P. gingivalis* more abundantly presented in biofilm in the presence of *Streptococcus gordonii* or *Streptococcus sanguinis* than *P. gingivalis* monospecies biofilm *in vitro* (Fig. 4E). Significantly more *P. gingivalis* colonization in the dual species than mono *P. gingivalis* biofilm was further confirmed through quantitative PCR (Fig. 4F).

Homeostatic IL-17-TRAF3IP2 Axis Strengthens Gingival Defense against Invading Oral Pathogens by Neutrophil Recruitment

We next performed a ligature-enhanced *P. gingivalis* local invasion experiment (Chipashvili et al. 2021). We found that gingiva from *Traf3ip2*$^{-/-}$ mice harbored significantly more total bacteria than WT mice prior to *P. gingivalis* challenge (Fig. 5A). We further detected a trend of more bacterial colonies in *Traf3ip2*$^{-/-}$ mouse gingival homogenate than WT mouse under an aerobic culture condition (Fig. 5B, Appendix Fig. 5). In *P. gingivalis*–challenged mice, the cultivatable bacterial colonies were significantly more in *Traf3ip2*$^{-/-}$ mouse gingival

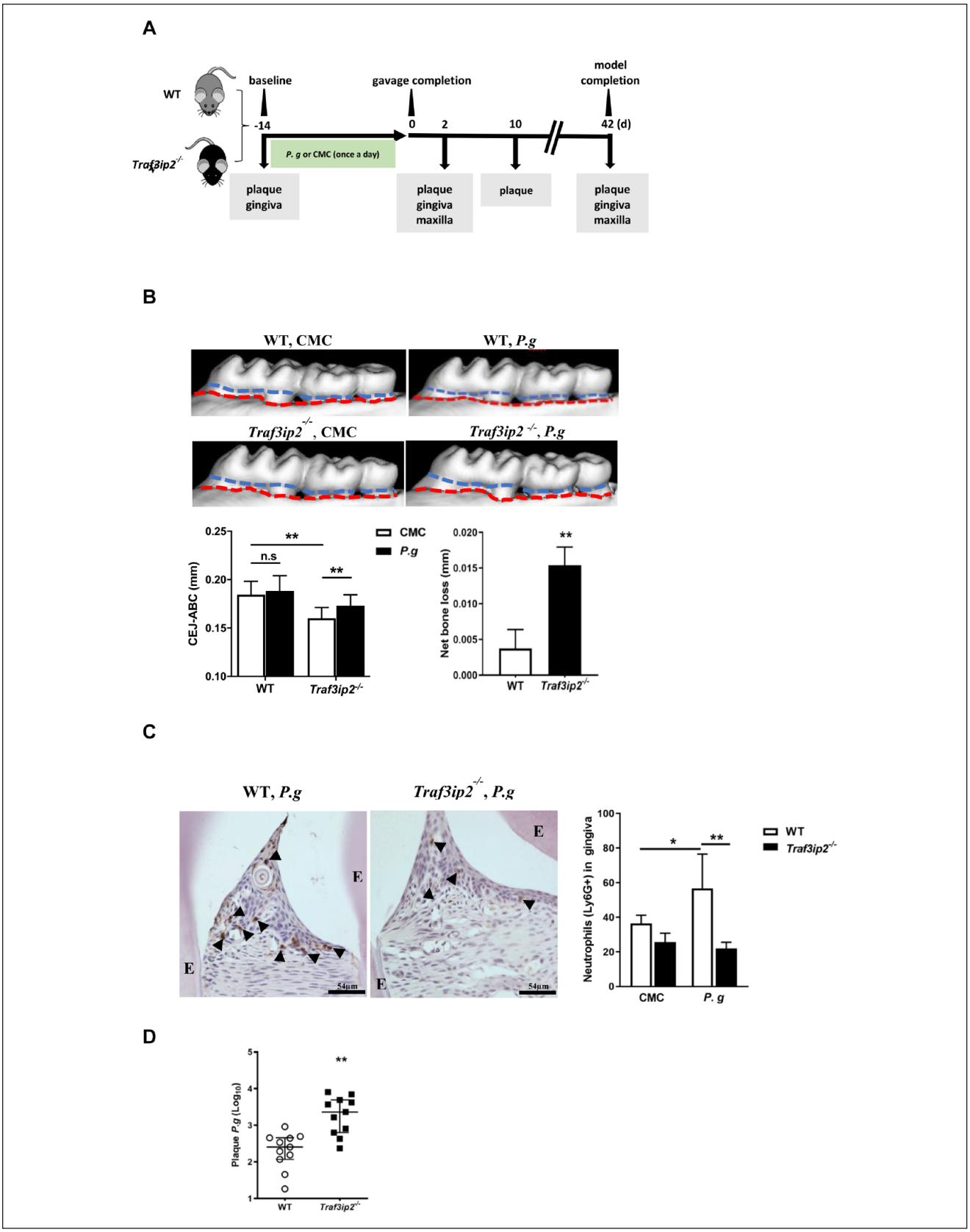

Figure 3. (continued)

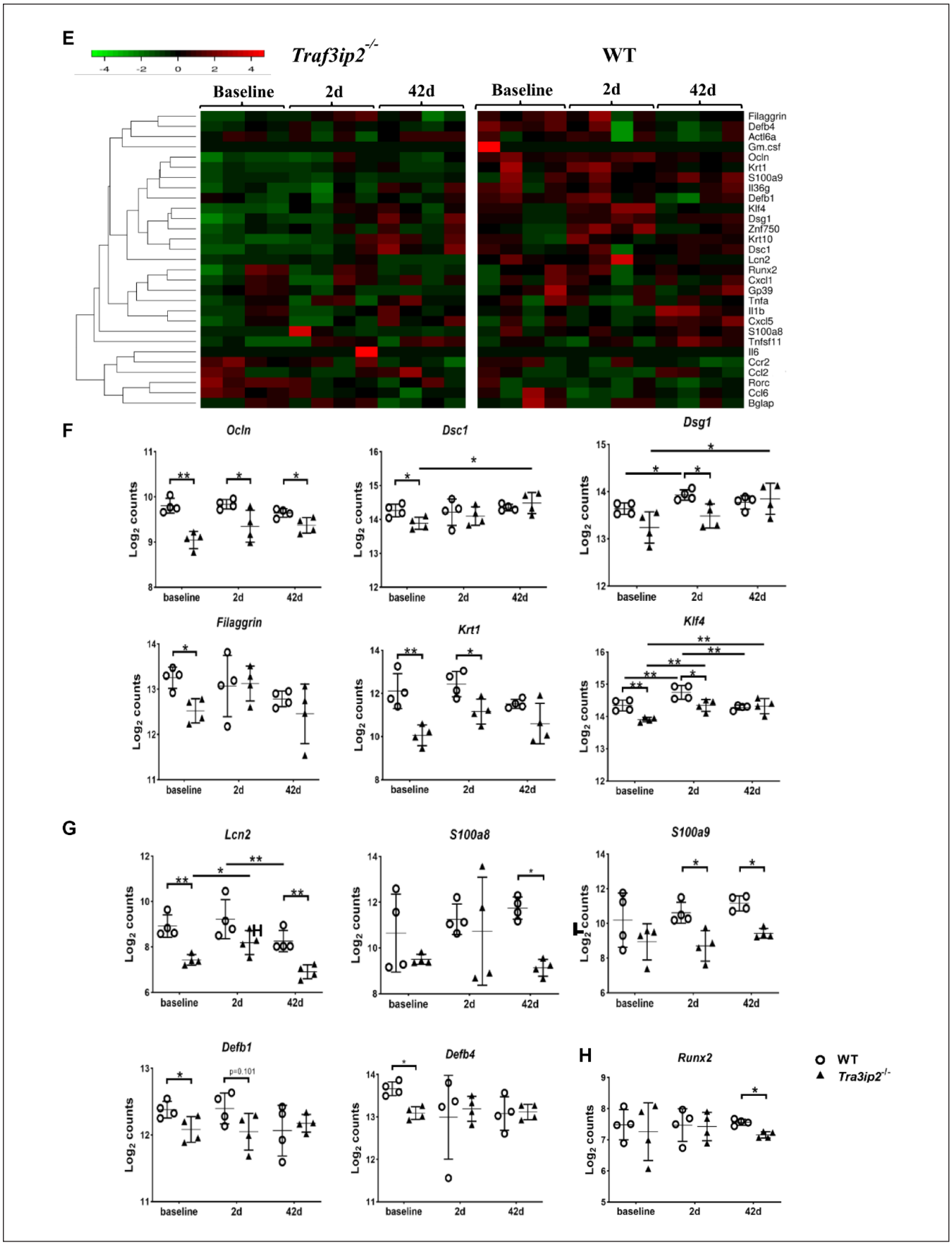

Figure 3. (continued)

Figure 3. *Traf3ip2*$^{-/-}$ mice were more susceptible to *Porphyromonas gingivalis*–induced periodontitis than wild-type (WT) mice. (**A**) WT and *Traf3ip2*$^{-/-}$ mice were orally challenged with either *P. gingivalis* A7436 (approximately 0.5×10^9 colony-forming units [CFUs]) or Carboxymethylcellulose CMC for 14 consecutive days. Maxillary bone was collected either 2 d or 42 d after the course of challenge. Gingival tissues and mouse oral plaque samples were also collected at different time points. (**B**, upper panel) Representative micro–computed tomography (μCT) images of alveolar bone loss measured from the cementoenamel junction (CEJ) (blue line) to the alveolar bone crest (ABC) (red line) for WT or *Traf3ip2*$^{-/-}$ mice that were orally challenged with *P. gingivalis* A7436 or CMC are shown. (**B**, lower left panel) The bone loss as represented by the distance between CEJ and ABC was compared between CMC and *P. gingivalis*–challenged WT mice or knockout mice. (**B**, lower right panel) The net bone loss between *P. gingivalis*– and CMC-challenged mice from *Traf3ip2*$^{-/-}$ mice was compared to WT mice. $n = 9$–10 mice/group; mean ± SEM is shown. (**C**) Neutrophils, which were Ly6G$^+$ stained by immunohistochemistry, as illustrated by arrowheads in the *P. gingivalis*–challenged *Traf3ip2*$^{-/-}$ mouse gingiva, were compared to WT mouse gingiva ($n = 3$–4/group). (**D**) Oral plaque was collected 2 d after the completion of *P.g* challenge and *P.g* CFUs were determined by quantitative polymerase chain reaction (qPCR) and compared between *Traf3ip2*$^{-/-}$ mice and WT mice ($n = 11$/group). Median and interquartile range are shown. (**E**) Murine gingival tissues were collected at baseline from unchallenged mice, 2 d and 42 d after *P.g* oral challenge. The NanoString transcriptomic gene expression associated with the neutrophil activation, epithelial function, and inflammatory response is presented by the heatmap. (**F**) Transcriptional expression of genes associated with epithelial function, (**G**) antimicrobial genes, and (**H**) *Runx2*, an osteoblast differentiation maker gene, as quantified by the NanoString analysis, was compared between WT and *Traf3ip2*$^{-/-}$ mouse gingiva at different time points in the course of *P.g* challenge. Bone loss and plaque *P. gingivalis* data were pooled from 2 independent experiments. $^*P < 0.05$; $^{**}P < 0.01$; $n = 4$ for both WT and *Traf3ip2*$^{-/-}$ mice at each time point for the NanoString transcriptomic analysis. Mean ± SD is shown.

homogenate than WT mice under both an aerobic and anaerobic condition (Fig. 5C). *P. gingivalis* DNA was present in 3 out of 10 *P. gingivalis*–challenged WT mouse gingival tissues in the invasion model, while 7 out of 10 *Traf3ip2*$^{-/-}$ mouse gingivae were clearly positive for *P. gingivalis* (Fig. 5D). More *P. gingivalis* invasion into *Traf3ip2*$^{-/-}$ gingiva was associated with significantly more bone loss in the distal root of the first molar than that of WT mice, although the bone loss in the mesial root of the second molar was not significantly different (Fig. 5E).

Based on the data in Figure 3C and G, we hypothesized that a dampened neutrophil response promoted *P. gingivalis* gingival invasion, leading to more severe bone loss observed in *Traf3ip2*$^{-/-}$ mice. To test this hypothesis, we depleted neutrophils in WT mice with the antibody 1A8 in the invasion model. The deletion efficiency was about 50% in gingiva and 65% in blood (Fig. 5F and Appendix Fig. 6A). We observed a trend of more cultivatable anaerobes in the gingival homogenate from the 1A8-treated mice than the isotype control antibody-treated animals after *P. gingivalis* challenge (Fig. 5G and Appendix Fig. 6B). While *P. gingivalis* DNA in the isotype antibody-treated mice was rarely detected, *P. gingivalis* DNA was found in all 6 gingival tissues collected from the neutrophil-depleted mice (Fig. 5H, left panel). Significantly more *P. gingivalis* invaded into the gingiva in neutrophil-depleted mice through quantitative polymerase chain reaction (qPCR) quantification (Fig. 5H, right panel). The 1A8-treated mice exhibited more alveolar bone loss than the isotype control antibody-treated mice (Fig. 5I). Overall, these data strongly suggest that the reduced neutrophil recruitment due to the absence of the TRAF3IP2-mediated IL-17 pathway in mouse gingiva permitted more *P. gingivalis* to invade into gingiva that resulted in more bone resorption.

Discussion

Recent studies frequently implicated an excess of IL-17 signaling in the pathogenesis of periodontitis. However, using *Traf3ip2*$^{-/-}$ mice simulating the extremity of a loss-of-function variant effect, we demonstrate that an integral IL-17–TRAF3IP2 signaling axis protects the host against the pathogen-induced periodontitis. Yu et al. (2007) reported that an absence of the IL-17 pathway in *Il17r(a)*$^{-/-}$ mice increased the animal's susceptibility to *P. gingivalis*–induced periodontitis. Therefore, fine-tuning the TRAF3IP2-mediated IL-17 response is fundamental to avoid the inflammatory insult while enhancing mucosal immune defense against invading periodontal pathogens.

Neutrophils patrolling at the mucosal surface play a pivotal role in defending mucosal barriers by eliminating invading pathogens (Conti et al. 2009; Hajishengallis et al. 2015; Uriarte et al. 2016). A reduced neutrophil recruitment to the gingiva in *Traf3ip2*$^{-/-}$ mice was associated with a delayed clearance of *P. gingivalis* and an increased local tissue invasion by this pathogen. The increased *P. gingivalis* inside the *Traf3ip2*$^{-/-}$ mouse gingiva was also possibly due to the pathogen retention in the unresolved periodontitis lesion. *P. gingivalis* A7436 is a virulent strain excelling at evasion of phagocytosis. This strain of *P. gingivalis* was shown to be notoriously persistent in cells upon invasion and a weak inducer of inflammation (Genco et al. 1991; Rodrigues et al. 2012). Our transcriptomic data also indicated that the *P. gingivalis* A7436 did not induce a more inflammatory response in *Traf3ip2*$^{-/-}$ than WT mice (Fig. 3E). However, a reduced neutrophil response in the *Traf3ip2* KO mice further aggravated the invasion by *P. gingivalis* A7436, a strain that is capable of "sneaking through" the mucosal defense barrier.

In this report, we used 3 murine models to assess the role of the TRAF3IP2–IL-17 axis in periodontitis. The widely used classical *P. gingivalis* oral challenge model, in which bone loss is usually moderate and slow progressing, mimics the overall host-specific pathogen interactions in human periodontitis. We found that a lack of neutrophil response was associated with more bone loss in *Traf3ip2*$^{-/-}$ mice upon *P. gingivalis* challenge. In the ligature-induced periodontitis model, which is fast-progressing and manifests more inflammation than the oral challenge model, the ligature promotes the aggregation of nonspecific plaque bacteria and amplifies gingival inflammatory responses. This model is typically used to evaluate the

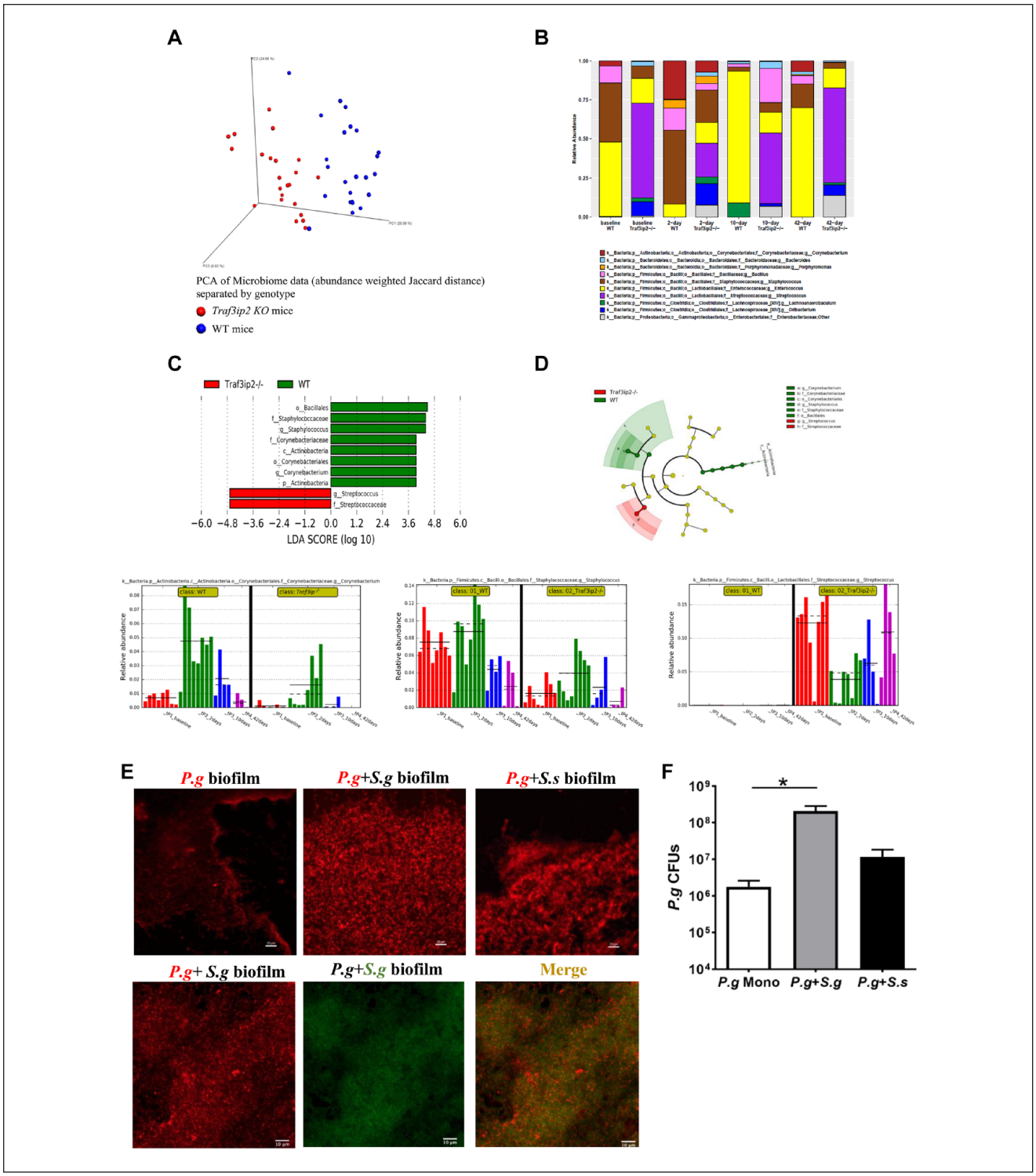

Figure 4. The oral plaque of *Traf3ip2*$^{-/-}$ mice harbored a unique microbial community structure. (**A**) A principal coordinate analysis (PCoA) of abundance-weighted Jaccard distance is shown to illustrate the β-diversity of murine oral plaque composition at different time points upon *Porphyromonas gingivalis* (*P.g*) challenge. (**B**) The average of the relative abundance from the top 10 most enriched plaque bacteria at the genus level is shown for each genotype of mice at different points upon *P.g* challenge. (**C**, upper panel) Differentially abundant taxonomic groups of bacteria with significance ($P<0.05$) and a linear discriminant analysis (LDA) score higher than 2.0 are shown. (**C**, lower panel) The relative abundance of plaque bacteria at the genus level that were significantly different between WT and *Traf3ip2*$^{-/-}$ mice is illustrated at different time points of the *P.g* oral challenge. (**D**) A cladogram illustrates differentially abundant taxonomic clades of plaque bacteria collected from either WT mice or *Traf3ip2*$^{-/-}$ mice. b, baseline prior to *P.g* challenge; tp, time point. (**E**) *P. gingivalis* (1×10^8 colony-forming units [CFU]/mL) was either monocultured or cocultured with *Streptococcus gordonii* (1×10^7 CFU/mL) or *Streptococcus sanguinis* (1×10^7 CFU/mL) in vitro to form biofilm on a cover slip. Eighteen hours after coculture, *P. gingivalis* or *S. gordonii* was probed by specific probes through fluorescence in situ hybridization. (**F**) *P.g* colonization in biofilm was quantified by qPCR. Data from 1 of 3 independent biofilm experiments are shown. *$P<0.05$. Scale bar represents 10 μm on top panel figures and 20 μm on lower panel figures. Mean ± SD is shown.

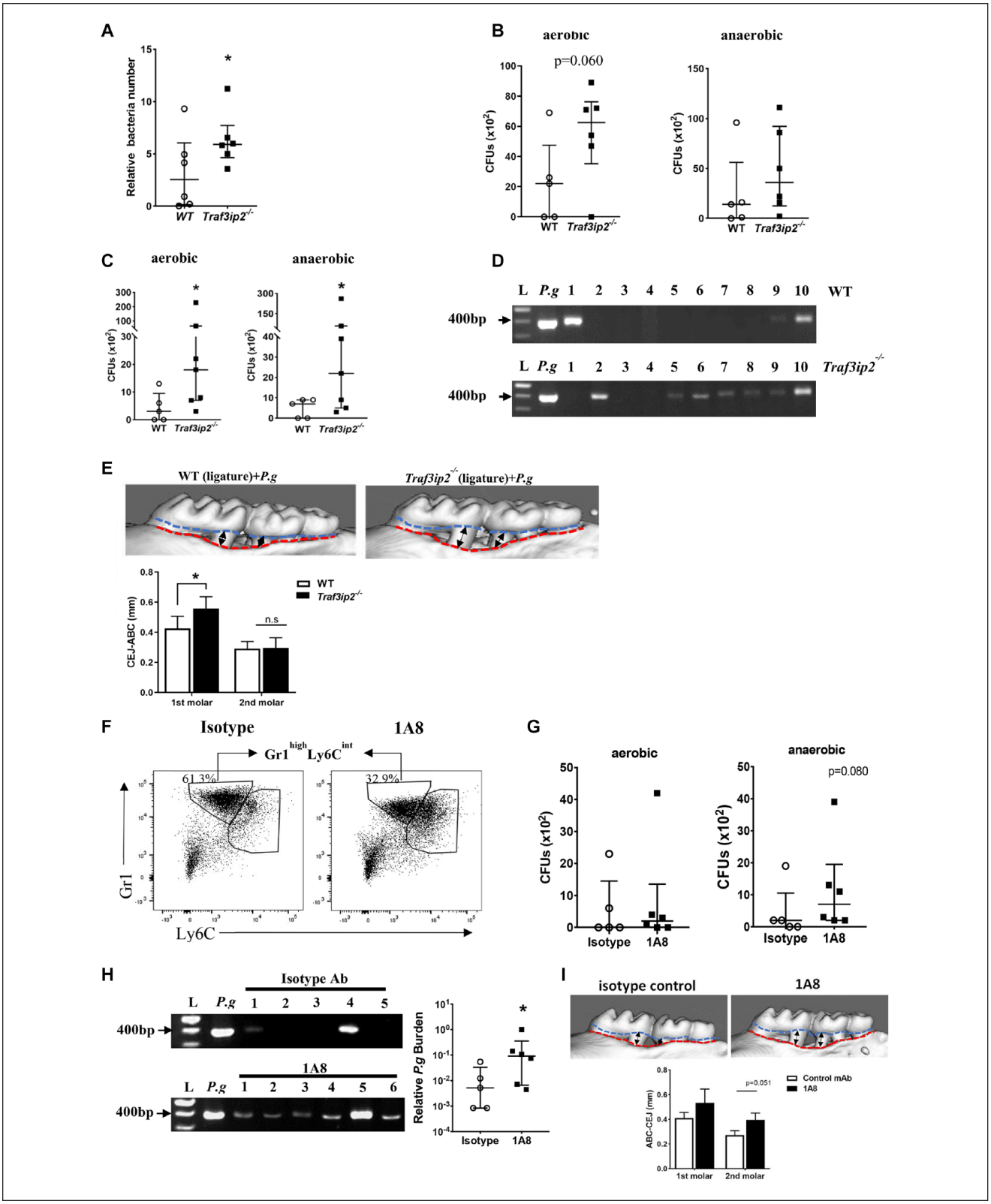

Figure 5. More bacteria invaded into the gingiva of *Traf3ip2*$^{-/-}$ mice than wild-type (WT) mice in the ligature-enhanced *Porphyromonas gingivalis* invasion model. After ligature placement, approximately 0.5×10^9 *P. gingivalis* or CMC carrier was applied to the mouse oral cavity. Such an oral challenge by *P.g* was repeated daily for 14 consecutive days. (**A**) The relative bacterial number from the gingival homogenate from which the animals were treated with CMC was compared by qPCR between WT and *Traf3ip2*$^{-/-}$ mice. (**B**) Bacterial colony-forming units (CFUs) were counted from those homogenates plated and cultured under either an aerobic or an anaerobic condition. (**C**) Bacterial CFUs were counted from the gingival homogenate collected from either WT or *Traf3ip2*$^{-/-}$ mice that were orally challenged with *P. gingivalis*. (**D**) *P. gingivalis* DNA was amplified by PCR and

host inflammatory response. However, the bone loss of *Traf3ip2*$^{-/-}$ mice in this model was not more severe than the WT mice (Appendix Fig. 3). A similar bone destruction in the *Traf3ip2*$^{-/-}$ mice to the WT mice suggests that the lack of IL-17 inflammatory response may be compensated by other inflammatory pathways such as the Toll-like receptor (TLR)–mediated immune response. Other immune cells than neutrophils, such as macrophages, also play a critical role in the bone loss in the ligature model (Sun et al. 2020). In the ligature-enhanced *P. gingivalis* invasion model, the ulceration of the sulcus epithelium induced by ligature facilitates more *P. gingivalis* intra-tissue invasion than the oral challenge alone (Graves et al. 2008). Combined with neutrophil depletion, this model allows us to study the specific role of neutrophils in *P. gingivalis* invasion. The inoculation of *P. gingivalis* in the invasion model promoted more anaerobic bacteria invasion and aggravated the bone loss in *Traf3ip2*$^{-/-}$ mice in comparison to WT mice. These data indicate that the local gingiva with a weak neutrophil-mediated barrier in *Traf3ip2*$^{-/-}$ mice is particular susceptible to the pathogenic bacteria such as *P. gingivalis*–induced bone loss. We also noted that the steady state of alveolar bone loss (CEJ–ABC) in *Traf3ip2*$^{-/-}$ mice was less than that of the WT mice (Fig. 3B). This is likely due to the fact that IL-17 is also an upstream bone resorption signal. It was shown that the loss of TRAF3IP2 had a protective effect for bone resorption in a non-infection post menopausal osteoporosis model (DeSelm et al. 2012).

Several GWA studies have identified novel candidate periodontitis-associating variants and genetic loci, most of which have not been previously implicated in periodontal disease (Divaris et al. 2013; Munz et al. 2017; Tong et al. 2019). Although neither the rs13190932 variant nor the rs33980500 variant was previously associated with periodontal disease, both variants have been repeatedly reported to be risk alleles for psoriasis and psoriatic arthritis (PA) in certain populations (Ellinghaus et al. 2010). Therefore, the shared variants identified by both periodontitis and psoriasis may suggest that the TRAF3IP2-mediated IL-17 pathway critically participates in the inflammatory response and barrier defense at mucocutaneous surfaces. Several clinical reports demonstrated that psoriasis or PA patients had more severe periodontal disease than subjects without psoriasis or PA (Skudutyte-Rysstad et al. 2014; Zhang et al. 2022). Therefore, the shared risk of periodontal disease and psoriasis modified by *TRAF3IP2* variants suggests a common etiopathogenic mechanism involving the IL-17–TRAF3IP2 axis that likely links oral and systemic diseases. Our data also suggested that a severe bone loss upon *P. gingivalis* challenge was associated with a compromised epithelial barrier. We found decreased transcription of several epithelial barrier and homeostatic marker genes in the *Traf3ip2*$^{-/-}$ gingiva without *P. gingivalis* challenge, indicating a potentially compromised epithelial barrier at the baseline level. Through RNA sequencing, Lambert et al. (2017) noted that the expression of several epithelial differentiation genes, including those that we reported here, was also downregulated in *TRAF3IP2*-silenced keratinocytes. Our data warrant further studies investigating the role of TRAF3IP2-mediated gingival epithelial barrier function in periodontitis.

We identified a less diverse microbial community structure in the oral plaque of *Traf3ip2*$^{-/-}$ mice than WT mice, which was associated with a decreased transcription of several antimicrobial genes in those mice. This finding contrasts several subgingival microbiome analyses in human subjects, which usually show a more diverse microbial community in periodontitis patients than periodontal health (Griffen et al. 2012; Camelo-Castillo et al. 2015). The dysbiotic pattern in *P. gingivalis*–induced periodontitis in a murine model may not be readily translatable to human periodontitis. A less diverse microbiome structure may be also inherently characteristic of a compromised gingival barrier in a reduced IL-17–TRAF3IP2–neutrophil response. Several studies have reported that mixed oral infection by *S. gordonii* and *P. gingivalis* in mice resulted in a more significant alveolar bone loss than *P. gingivalis* monoinfection (Daep et al. 2011; Kuboniwa et al. 2017). The more abundant *Streptococcus* bacteria in *Traf3ip2*$^{-/-}$ mouse oral plaque may drastically enhance the plaque biofilm colonization by *P. gingivalis* (Maeda et al. 2008; Daep et al. 2011).

We acknowledge that the findings of this study might be limited to the A7436 strain of *P. gingivalis*. Other commonly used strains need to be tested to confirm whether the homeostatic IL-17–TRAF3IP2–mediated immune response is a common mechanism to enhance mucosal defense. However, based on the similar biological structure and behavior of A7436 to other strains such as W83, we would expect that the disease mechanism identified using the A7436 strain in our models can be generalizable to other *P. gingivalis* strains (Chastain-Gross et al. 2015).

In summary, we demonstrated that the lead exonic variant rs13190932, which is likely a surrogate SNP for a genuine loss-of-function variant rs33980500, within the *TRAF3IP2* locus was significantly associated with more severe periodontitis in carriers with a high microbial pathogen burden than noncarriers. Animal model data further delineated an essential role of the IL-17–TRAF3IP2–neutrophil axis in safeguarding the gingival immune barrier against *P. gingivalis* invasion and

shown in electrophoresis from the gingival homogenate collected from the pathogen-challenged WT or *Traf3ip2*$^{-/-}$ mice. "L" indicates a DNA ladder; "*P.g*" indicates a positive control of *P. gingivalis* DNA. (**E**) Alveolar bone loss at the first and second maxillary molar in the ligature-enhanced invasion model from *Traf3ip2*$^{-/-}$ mice was compared to WT mice. (**F**) Representative fluorescence-activated cell sorting (FACS) plots from a representative experiment show the neutrophil ($CD45^+CD11b^+Gr1^+Ly6C^{int}$) population in gingiva collected from either isotype control or 1A8-treated mice. (**G**) Colonies were counted from the plated gingival homogenate under either an aerobic or an anaerobic condition from the animals after *P. gingivalis* challenge in the invasion model. (**H**) DNA was isolated from the gingival homogenate and amplified through PCR to detect *P. gingivalis.* The *P. gingivalis* burden was determined by qPCR against the standard titration curve of *P. gingivalis*. (**I**) Maxillae were scanned through micro–computed tomography, and the alveolar bone loss of the maxillary first and second molars was compared in animals treated with either isotype control or 1A8 antibody. Median ± interquartile range is shown for bacteria quantification, while mean ± SD is shown for bone loss. Data were pooled from at least 2 independent experiments ($n = 5–10$/group). *$P < 0.05$.

therefore mitigating the *P. gingivalis*–induced alveolar bone loss. In addition, the loss of TRAF3IP2 in mice was characteristically associated with a distinct oral microbial community structure.

Author Contributions

J. Zhang, L. Sun, contributed to design, data analysis, drafted and critically revised the manuscript; M.H.H. Withanage, contributed to data analysis, drafted and critically revised the manuscript; S.M. Ganesan, F.R. Teles, contributed to data analysis and interpretation, critically revised the manuscript; M.A. Williamson, contributed to data acquisition and analysis, critically revised the manuscript; J.T. Marchesan, contributed to conception, data analysis, critically revised the manuscript; Y. Jiao, contributed to conception, data acquisition, critically revised the manuscript; N. Yu, contributed to data acquisition and interpretation, critically revised the manuscript; Y. Liu, D. Wu, K.L. Moss, contributed to data analysis, critically revised the manuscript; A.K. Mangalam, Y.L. Lei, contributed to data conception, critically revised the manuscript; E. Zeng, contributed to data analysis and interpretation, drafted the manuscript; S. Zhang, contributed to conception and design, data acquisition, analysis, and interpretation, drafted and critically revised the manuscript. All authors gave final approval and agree to be accountable for all aspects of the work.

Acknowledgments

The Atherosclerosis Risk in Communities (ARIC) Study is carried out as a collaborative study supported by National Heart, Lung, and Blood Institute contracts (HHSN268201100005C, HHSN268201100006C, HHSN268201100007C, HHSN26820 1100008C, HHSN268201100009C, HHSN268201100010C, HHSN268201100011C, and HSN268201100012C), R01HL 087641, R01HL59367, and R01HL086694; National Human Genome Research Institute contract U01HG004402; National Institutes of Health (NIH) contract HHSN268200625226C; National Institute of Environmental Health Sciences grant P30ES010126; and National Institute of Dental and Craniofacial Research grants R01DE11551 and R01DE021418. We deeply thank the staff and participants of the ARIC study for their contributions. We thank Dr. Ulrich Siebenlist at the National Institute of Allergy and Infectious Diseases for providing *Traf3ip2(Act1, CISK)*$^{-/-}$ and wild-type control animals. We also thank the Center for Gastrointestinal Biology and Disease (CGIBD P30 DK034987) and the UNC Nutrition Obesity Research Center (NORC P30 DK056350). We want to recognize Dr. Steven Offenbacher, a pioneer in periodontal research whose leadership and expertise contributed to the early conceptualization of this research. The data presented herein were obtained at the Flow Cytometry Facility, which is a Carver College of Medicine/Holden Comprehensive Cancer Center core research facility at the University of Iowa. The facility is funded through user fees and the generous financial support of the Carver College of Medicine, Holden Comprehensive Cancer Center, and Iowa City Veteran's Administration Medical Center.

Declaration of Conflicting Interests

The authors declared no potential conflicts of interest with respect to the research, authorship, and/or publication of this article.

Funding

The authors disclosed receipt of the following financial support for the research, authorship, and/or publication of this article: This research was funded by NIH grants R00 DE027086 (to S.Z.), K01 DE027087 (to J.T.M.), R01 DE026728 and U01 DE029255 (to Y.L.L.), and F32 DE026688 (Y.J.).

ORCID iD

J.T. Marchesan https://orcid.org/0000-0003-0610-3193

Data Availability

All data published in this article are available upon reasonable request.

References

Baker PJ, Dixon M, Roopenian DC. 2000. Genetic control of susceptibility to *Porphyromonas gingivalis*-induced alveolar bone loss in mice. Infect Immun. 68(10):5864–5868.

Boisson B, Wang C, Pedergnana V, Wu L, Cypowyj S, Rybojad M, Belkadi A, Picard C, Abel L, Fieschi C, et al. 2013. An ACT1 mutation selectively abolishes interleukin-17 responses in humans with chronic mucocutaneous candidiasis. Immunity. 39(4):676–686.

Camelo-Castillo AJ, Mira A, Pico A, Nibali L, Henderson B, Donos N, Tomas I. 2015. Subgingival microbiota in health compared to periodontitis and the influence of smoking. Front Microbiol. 6:119.

Chastain-Gross RP, Xie G, Belanger M, Kumar D, Whitlock JA, Liu L, Farmerie WG, Daligault HE, Han CS, Brettin TS, et al. 2015. Genome sequence of *Porphyromonas gingivalis* strain A7436. Genome Announc. 3(5):e00927-15.

Chipashvili O, Utter DR, Bedree JK, Ma Y, Schulte F, Mascarin G, Alayyoubi Y, Chouhan D, Hardt M, Bidlack F, et al. 2021. Episymbiotic saccharibacteria suppresses gingival inflammation and bone loss in mice through host bacterial modulation. Cell Host Microbe. 29(11):1649–1662.e7.

Ciccacci C, Biancone L, Di Fusco D, Ranieri M, Condino G, Giardina E, Onali S, Lepre T, Pallone F, Novelli G, et al. 2013. TRAF3IP2 gene is associated with cutaneous extraintestinal manifestations in inflammatory bowel disease. J Crohns Colitis. 7(1):44–52.

Conti HR, Shen F, Nayyar N, Stocum E, Sun JN, Lindemann MJ, Ho AW, Hai JH, Yu JJ, Jung JW, et al. 2009. Th17 cells and IL-17 receptor signaling are essential for mucosal host defense against oral candidiasis. J Exp Med. 206(2):299–311.

Daep CA, Novak EA, Lamont RJ, Demuth DR. 2011. Structural dissection and in vivo effectiveness of a peptide inhibitor of *Porphyromonas gingivalis* adherence to *Streptococcus gordonii*. Infect Immun. 79(1):67–74.

DeSelm CJ, Takahata Y, Warren J, Chappel JC, Khan T, Li X, Liu C, Choi Y, Kim YF, Zou W, et al. 2012. IL-17 mediates estrogen-deficient osteoporosis in an Act1-dependent manner. J Cell Biochem. 113(9):2895–2902.

Divaris K, Monda KL, North KE, Olshan AF, Reynolds LM, Hsueh WC, Lange EM, Moss K, Barros SP, Weyant RJ, et al. 2013. Exploring the genetic basis of chronic periodontitis: a genome-wide association study. Hum Mol Genet. 22(11):2312–2324.

Ellinghaus E, Ellinghaus D, Stuart PE, Nair RP, Debrus S, Raelson JV, Belouchi M, Fournier H, Reinhard C, Ding J, et al. 2010. Genome-wide association study identifies a psoriasis susceptibility locus at TRAF3IP2. Nat Genet. 42(11):991–995.

Genco CA, Cutler CW, Kapczynski D, Maloney K, Arnold RR. 1991. A novel mouse model to study the virulence of and host response to *Porphyromonas* (bacteroides) *gingivalis*. Infect Immun. 59(4):1255–1263.

Graves DT, Fine D, Teng YT, Van Dyke TE, Hajishengallis G. 2008. The use of rodent models to investigate host-bacteria interactions related to periodontal diseases. J Clin Periodontol. 35(2):89–105.

Griffen AL, Beall CJ, Campbell JH, Firestone ND, Kumar PS, Yang ZK, Podar M, Leys EJ. 2012. Distinct and complex bacterial profiles in human periodontitis and health revealed by 16S pyrosequencing. ISME J. 6(6):1176–1185.

Gu C, Wu L, Li X. 2013. IL-17 family: cytokines, receptors and signaling. Cytokine. 64(2):477–485.

Ha HL, Wang H, Pisitkun P, Kim JC, Tassi I, Tang W, Morasso MI, Udey MC, Siebenlist U. 2014. IL-17 drives psoriatic inflammation via distinct, target cell-specific mechanisms. Proc Natl Acad Sci U S A. 111(33):E3422–E3431.

Hajishengallis G, Chavakis T, Hajishengallis E, Lambris JD. 2015. Neutrophil homeostasis and inflammation: novel paradigms from studying periodontitis. J Leukoc Biol. 98(4):539–548.

Huang F, Kao CY, Wachi S, Thai P, Ryu J, Wu R. 2007. Requirement for both JAK-mediated PI3K signaling and ACT1/TRAF6/TAK1-dependent NF-kappaB activation by IL-17A in enhancing cytokine expression in human airway epithelial cells. J Immunol. 179(10):6504–6513.

Hüffmeier U, Uebe S, Ekici AB, Bowes J, Giardina E, Korendowych E, Juneblad K, Apel M, McManus R, Ho P, et al. 2010. Common variants at TRAF3IP2 are associated with susceptibility to psoriatic arthritis and psoriasis. Nat Genet. 42(11):996–999.

Kuboniwa M, Houser JR, Hendrickson EL, Wang Q, Alghamdi SA, Sakanaka A, Miller DP, Hutcherson JA, Wang T, Beck DAC, et al. 2017. Metabolic crosstalk regulates *Porphyromonas gingivalis* colonization and virulence during oral polymicrobial infection. Nat Microbiol. 2(11):1493–1499.

Lambert S, Swindell WR, Tsoi LC, Stoll SW, Elder JT. 2017. Dual role of Act1 in keratinocyte differentiation and host defense: TRAF3IP2 silencing alters keratinocyte differentiation and inhibits IL-17 responses. J Invest Dermatol. 137(7):1501–1511.

Maeda K, Tribble GD, Tucker CM, Anaya C, Shizukuishi S, Lewis JP, Demuth DR, Lamont RJ. 2008. A *Porphyromonas gingivalis* tyrosine phosphatase is a multifunctional regulator of virulence attributes. Mol Microbiol. 69(5):1153–1164.

Marujo F, Pelham SJ, Freixo J, Cordeiro AI, Martins C, Casanova JL, Lei WT, Puel A, Neves JF. 2021. A novel TRAF3IP2 mutation causing chronic mucocutaneous candidiasis. J Clin Immunol. 41(6):1376–1379.

Munz M, Willenborg C, Richter GM, Jockel-Schneider Y, Graetz C, Staufenbiel I, Wellmann J, Berger K, Krone B, Hoffmann P, et al. 2017. A genome-wide association study identifies nucleotide variants at SIGLEC5 and DEFA1A3 as risk loci for periodontitis. Hum Mol Genet. 26(13):2577–2588.

Myers TA, Chanock SJ, Machiela MJ. 2020. *LDlinkR*: an R package for rapidly calculating linkage disequilibrium statistics in diverse populations. Front Genet. 11:157.

Offenbacher S, Divaris K, Barros SP, Moss KL, Marchesan JT, Morelli T, Zhang S, Kim S, Sun L, Beck JD, et al. 2016. Genome-wide association study of biologically informed periodontal complex traits offers novel insights into the genetic basis of periodontal disease. Hum Mol Genet. 25(10):2113–2129.

Rodrigues PH, Reyes L, Chadda AS, Belanger M, Wallet SM, Akin D, Dunn W Jr, Progulske-Fox A. 2012. *Porphyromonas gingivalis* strain specific interactions with human coronary artery endothelial cells: a comparative study. PLoS One. 7(12):e52606.

Simionato MR, Tucker CM, Kuboniwa M, Lamont G, Demuth DR, Tribble GD, Lamont RJ. 2006. *Porphyromonas gingivalis* genes involved in community development with *Streptococcus gordonii*. Infect Immun. 74(11):6419–6428.

Skudutyte-Rysstad R, Slevolden EM, Hansen BF, Sandvik L, Preus HR. 2014. Association between moderate to severe psoriasis and periodontitis in a Scandinavian population. BMC Oral Health. 14:139.

Sønder SU, Paun A, Ha HL, Johnson PF, Siebenlist U. 2012. CIKS/Act1-mediated signaling by IL-17 cytokines in context: implications for how a CIKS gene variant may predispose to psoriasis. J Immunol. 188(12):5906–5914.

Sun L, Girnary M, Wang L, Jiao Y, Zeng E, Mercer K, Zhang J, Marchesan JT, Yu N, Moss K, et al. 2020. IL-10 dampens an IL-17-mediated periodontitis-associated inflammatory network. J Immunol. 204(8):2177–2191.

Tong H, Wei Z, Yin J, Zhang B, Zhang T, Deng C, Huang Y, Zhang N. 2019. Genetic susceptibility of common polymorphisms in NIN and SIGLEC5 to chronic periodontitis. Sci Rep. 9(1):2088.

Uriarte SM, Edmisson JS, Jimenez-Flores E. 2016. Human neutrophils and oral microbiota: a constant tug-of-war between a harmonious and a discordant coexistence. Immunol Rev. 273(1):282–298.

Wang C, Wu L, Bulek K, Martin BN, Zepp JA, Kang Z, Liu C, Herjan T, Misra S, Carman JA, et al. 2013. The psoriasis-associated D10N variant of the adaptor Act1 with impaired regulation by the molecular chaperone hsp90. Nat Immunol. 14(1):72–81.

Wu L, Wang C, Boisson B, Misra S, Rayman P, Finke JH, Puel A, Casanova JL, Li X. 2014. The differential regulation of human ACT1 isoforms by Hsp90 in IL-17 signaling. J Immunol. 193(4):1590–1599.

Yu JJ, Ruddy MJ, Wong GC, Sfintescu C, Baker PJ, Smith JB, Evans RT, Gaffen SL. 2007. An essential role for IL-17 in preventing pathogen-initiated bone destruction: recruitment of neutrophils to inflamed bone requires IL-17 receptor-dependent signals. Blood. 109(9):3794–3802.

Zhang S, Yu N, Arce RM. 2020. Periodontal inflammation: integrating genes and dysbiosis. Periodontol 2000. 82(1):129–142.

Zhang X, Gu H, Xie S, Su Y. 2022. Periodontitis in patients with psoriasis: a systematic review and meta-analysis. Oral Dis. 28(1):33–43.